Published online: June 13, 2014

Scientific Report

TRANSPARENT PROCESS

EMBO reports

Genetically encoded impairment of neuronal KCC2 cotransporter function in human idiopathic generalized epilepsy

Kristopher T Kahle[1,2,†], Nancy D Merner[3,4,†], Perrine Friedel[5,6], Liliya Silayeva[7], Bo Liang[8], Arjun Khanna[2], Yuze Shang[1,2], Pamela Lachance-Touchette[9], Cynthia Bourassa[9], Annie Levert[4], Patrick A Dion[3,10], Brian Walcott[2], Dan Spiegelman[4], Alexandre Dionne-Laporte[4], Alan Hodgkinson[11], Philip Awadalla[11,12], Hamid Nikbakht[13], Jacek Majewski[13], Patrick Cossette[9], Tarek Z Deeb[7], Stephen J Moss[7], Igor Medina[5,6] & Guy A Rouleau[4,*]

Abstract

The KCC2 cotransporter establishes the low neuronal Cl^- levels required for $GABA_A$ and glycine (Gly) receptor-mediated inhibition, and KCC2 deficiency in model organisms results in network hyperexcitability. However, no mutations in KCC2 have been documented in human disease. Here, we report two non-synonymous functional variants in human KCC2, R952H and R1049C, exhibiting clear statistical association with idiopathic generalized epilepsy (IGE). These variants reside in conserved residues in the KCC2 cytoplasmic C-terminus, exhibit significantly impaired Cl^--extrusion capacities resulting in less hyperpolarized Gly equilibrium potentials (E_{Gly}), and impair KCC2 stimulatory phosphorylation at serine 940, a key regulatory site. These data describe a novel KCC2 variant significantly associated with a human disease and suggest genetically encoded impairment of KCC2 functional regulation may be a risk factor for the development of human IGE.

Keywords cation-chloride cotransporters; epilepsy; GABA; KCC2; kinase
Subject Categories Molecular Biology of Disease; Neuroscience; Membrane & Intracellular Transport
DOI 10.15252/embr.201438840 | Received 27 March 2014 | Revised 18 April 2014 | Accepted 23 April 2014 | Published online 13 June 2014
EMBO Reports (2014) 15: 766–774
See also: **M Puskarjov *et al*** (June 2014) and **CA Hübner** (July 2014)

Introduction

The K^+-Cl^- cotransporter KCC2 (*SLC12A5*) is the main Cl^- extrusion mechanism in mature neurons and is essential for type A GABA ($GABA_A$) and glycine (Gly) receptor-mediated Cl^- currents underlying fast synaptic inhibition [1]. KCC2 deficiency in model organisms results in network hyperexcitability [2–6]. KCC2 functional down-regulation has been implicated in neurological disorders featuring GABAergic disinhibition [7]. However, no mutations in KCC2 have been described in human disease.

The idiopathic generalized epilepsies (IGEs) are primarily genetic in origin and include rare Mendelian diseases and more common familial forms which manifest as complex traits [8]. However, the genetic architecture of IGE is not well understood. A recent exome-sequencing study attempted to identify IGE variants of large effect by taking a variant-based approach and performing large-scale genotyping on selected rare exome-sequencing variants [9]. Individual variants contributing significantly to disease were not identified because, as the authors noted, the impact of any individual single-nucleotide variant in IGE is small. A gene-based approach seeking multiple rare alleles within the same gene might be an alternative approach for identifying genetic risk factors for IGE [9].

The cytoplasmic C-terminus of KCC2 is an important regulatory region of transporter function [reviewed in 1, 10–12; e.g., 13] (Fig 1). We employed a targeted DNA-sequencing approach to screen this region in KCC2 (amino acids 894 1086; NP_065759),

1 Department of Cardiology, Manton Center for Orphan Disease Research, Howard Hughes Medical Institute, Boston Children's Hospital, Boston, MA, USA
2 Department of Neurosurgery, Massachusetts General Hospital, Boston, MA, USA
3 Department of Drug Discovery and Development, Harrison School of Pharmacy, Auburn University, Auburn, AL, USA
4 Department of Neurology and Neurosurgery, Montreal Neurological Hospital and Institute, McGill Université, Montréal, QC, Canada
5 INMED, INSERM Unité 901, Marseille, France
6 Aix-Marseille Université, UMR 901, Marseille, France
7 Department of Neuroscience, Tufts University School of Medicine, Boston, MA, USA
8 Department of Biological Chemistry and Molecular Pharmacology (BCMP), Harvard Medical School, Boston, MA, USA
9 Center of Research of the Université de Montréal and the Department of Medicine, Université de Montréal, Montréal, QC, Canada
10 Department of Pathology and Cell Biology, Université de Montréal, Montréal, QC, Canada
11 CHU Sainte Justine Research Centre, Department of Pediatrics, Faculty of Medicine, Université de Montréal, Montréal, QC, Canada
12 CARTaGENE, Montréal, QC, Canada
13 Department of Human Genetics, McGill University and Genome Quebec Innovation Centre, Montréal, QC, Canada
*Corresponding author. Tel: +1 514 890 8000 ext. 24699; E-mail: guy.rouleau@mcgill.ca
†These authors contributed equally to this work.

along with the homologous region in KCC3 (*SLC12A6*) (amino acids 979 1570; NP_598408), and the N-terminal regulatory region in NKCC1 (*SLC12A2*) [14,15] (amino acids 150 252; NP_001037) for genetic variations in a 380-patient French-Canadian cohort of IGE (see Supplementary Methods). We hypothesized functionally relevant genetic variation in these regions might alter transporter activity and contribute to IGE by altering neuronal Cl^- homeostasis, and consequently, GABA/glycine activity.

Results

After Sanger sequencing the C-terminus of KCC2, an enrichment of non-synonymous (NS) alleles was discovered in IGE cases compared to controls (Table 1; see Supplementary Methods for IGE clinical details). A trend was first noticed when comparing the total number of NS alleles identified in IGE cases (n = 8/760) to Quebec controls (n = 2/950; P = 0.028; Table 1). In order to validate this association, an additional 739 Quebec controls were screened, bringing the total number of control alleles to 2428. A total of 6 NS alleles were detected in the control cohort (n = 6/2428), improving the P-value to 7.50×10^{-3} (Table 1). When considering the total number of C-terminal NS alleles that were identified in the European American (EA) cohort from the Exome Variant Server (EVS), a P-value of 2.2×10^{-4} was generated. The P-value became more significant when all EVS alleles were considered ($P = 7.7 \times 10^{-5}$; Supplementary Table S1). Overall, NS alleles in this important regulatory region are associated with IGE. Specifically, two different NS KCC2

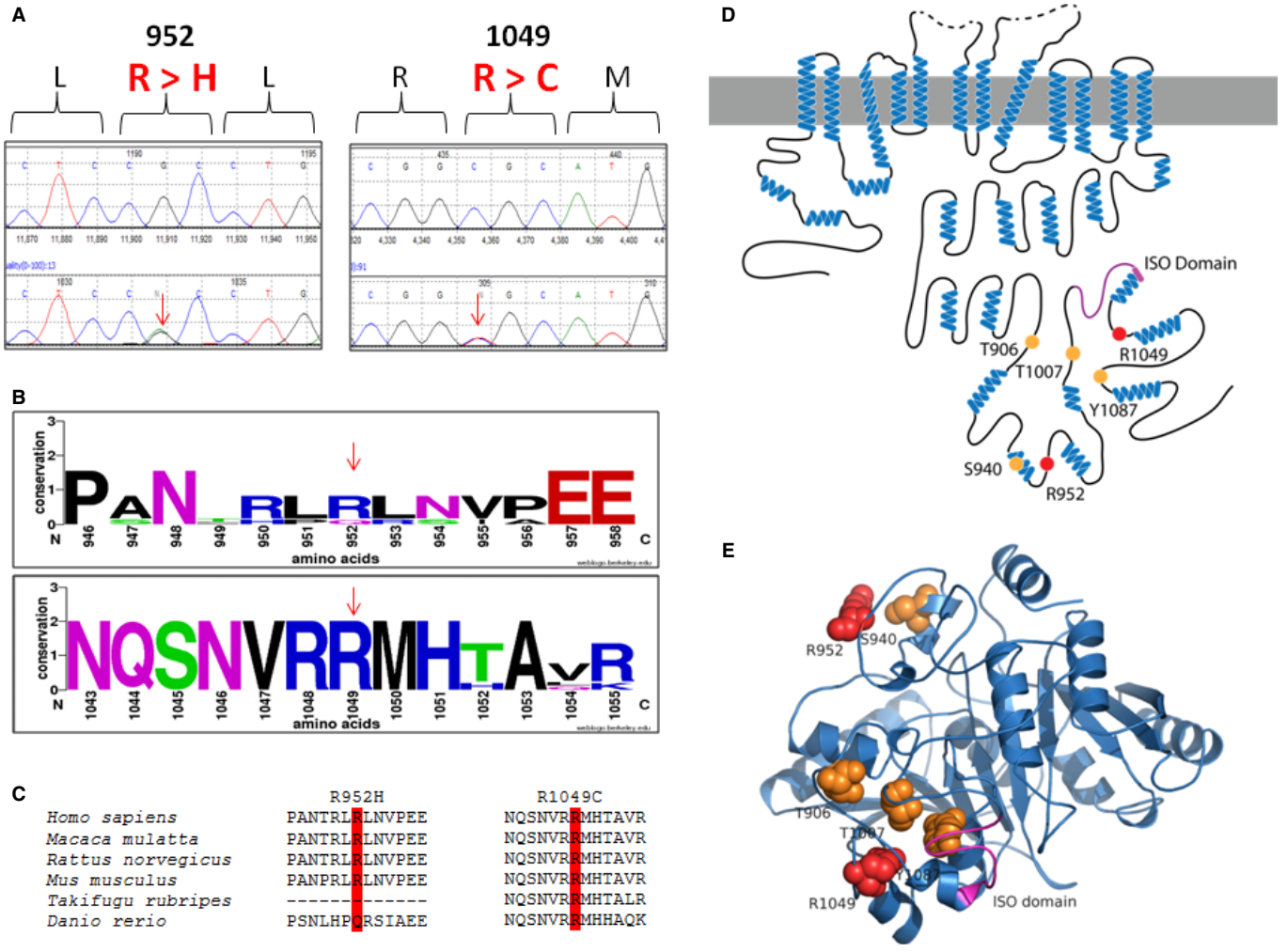

Figure 1. Identified *KCC2* (*SLC12A5*) variants in human IGE.

A DNA chromatograms illustrating the detection of c.2855 G > A (p.R952H) and c.3145 C > T (p.R1049C) via Sanger sequencing.

B, C Evolutionary conservation of amino acids p.R952 and p.R1049.

D Schematic representation of KCC2 (human). Orange dots indicate the positions of the known critical phospho-regulatory residues p.T906, p.S940, p.T1007, and p.Y1087 (reviewed in [10]). Pink region denotes the KCC2 'ISO' domain, required for hyperpolarizing GABAergic transmission [13]. Red dots depict the two identified IGE mutations, p.R952 and p.R1049.

E The modeled structure of the human KCC2 C-terminal domain, based on homology modeling by I-TASSER using a prokaryotic member of the cation-chloride cotransporter family (PDB code 3g40) (see Materials and Methods for details). Color scheme same as in (D). Note the proximity of the KCC2 IGE variants to important regulatory residues and domains.

Published online: June 13, 2014
EMBO reports

Table 1. KCC2 (*SLC12A5*) variants detected in the IGE cohort.

Non-synonymous variants detected in the 'hotspot'		Detection of variants in IGE cohort			Control data							
					Quebec population controls (Phase 1: 475 controls)				Quebec population controls (Total: 1,214 controls)			
mRNA (NM_020708.4)	Protein (NP_065759)	Number of probands	Number of alleles	Allele frequency (%)	Number of alleles	Allele frequency (%)	*P*-value	Odds ratio	Number of alleles	Allele frequency (%)	*P*-value	Odds ratio
c.2855 G>A	p.R952H	5/380	5/760	0.66	2/950	0.21	0.253	3.14 CI_{95} [0.5–33.0]	5/2,428	0.21	0.065	3.21 CI_{95} [0.7–14.0]
c.3145 C>T	p.R1049C	3/380	3/760	0.39	0/950	0.00	0.088	Inf CI_{95} [0.5-Inf]	1/2,428	4.12×10^{-4}	0.044	9.61 CI_{95} [0.8–503.6]
Total number of non-synonymous alleles detected		8/380	8/760	–	2/950	–	0.028	5.04 CI_{95} [1.0–48.8]	6/2,428	–	7.50×10^{-3}	4.29 CI_{95} [1.3–15.1]

variants were identified, R1049C and R952H (Fig 1 and Table 1). All variants were heterozygous.

R1049C is a novel KCC2 variant detected in 3 of the 380 IGE cases (Table 1; Supplementary Table S2). This variant is previously unreported and was not detected in the first 950 Quebec alleles that were screened but was detected in one of the 2428 Quebec control alleles (Table 1). This extremely rare variant is enriched in our IGE cohort ($P = 0.044$; Table 1). Furthermore, R1049 is a highly conserved residue (Fig 1), and a substitution for a cysteine at that position is predicted to be highly pathogenic using multiple *in silico* bioinformatics programs (Table 2). Moreover, the parental DNA was available for two of the three probands with R1049C. In both cases, the parents were unaffected, and the variant was maternally inherited.

The R952H variant was detected in five IGE cases, corresponding to an allele frequency of 0.66% (Table 1; Supplementary Table S2). After screening the first 950 control alleles, an allele frequency of 0.21% was determined ($P = 0.253$). The same allele frequency was calculated upon increasing the number of control alleles to 2428, which improved the *P*-value to 0.065 (Table 1). This rare variant appears to be more frequent in Quebec than in other populations; for example, it is reported in only 0.07% of EA alleles and 0.05% of all alleles on the EVS (Supplementary Table S1). Nevertheless, R952H is enriched in these Quebec IGE cases compared to Quebec controls. R952 shows strong evolutionary conservation (Fig 1), and histidine substitution at this site is predicted to have deleterious effects on protein function (Table 2). Thus, similar to R1049C, R952H appears to be an IGE risk variant. Furthermore, DNA was available from the parents of three probands with R952H, all of which were unaffected. The variant was inherited in all cases (maternally in two and paternally in one case).

KCC3 and NKCC1, CCCs like KCC2, have been implicated in seizures in humans and model organisms [16–20]. Given the conservation of regulatory mechanisms regulating the CCCs [21–23], we screened these regions of KCC3 and NKCC1 in our IGE patient cohort (see Supplementary Methods for details). No KCC3 or NKCC1 coding variants were detected, thereby highlighting the specificity of the association of KCC2 variation with human IGE.

We next determined whether the identified IGE variants affect KCC2 function by recording the reversal potential of glycine receptors (GlyR, E_{Gly}), which is principally determined by intracellular Cl^- concentration ($[Cl^-]_i$). GlyRs were co-expressed with IGE KCC2 variant or WT KCC2 in N2a cells. To visualize cells expressing different KCC2 species, all KCC2 constructs were conjugated at their N-termini with mCherry fluorescent protein (mCherry-KCC2) (Fig 2A) [24]. Using the gramicidin-perforated patch-clamp technique, we found that cells expressing mCherry-KCC2 exhibited a strong shift in E_{Gly} toward negative (more hyperpolarized) values compared to controls (Fig 2B,C; -38.1 ± 3.7 mV and -89.4 ± 3.2, respectively, see Supplementary Table S3). mCherry-$KCC2_{R1049C}$ and mCherry-$KCC2_{R952H}$ also produced a hyperpolarizing shift of E_{Gly}; however, the absolute values were more positive (i.e., less hyperpolarized) compared to WT mCherry-KCC2 (Fig 2C). The difference between E_{Gly} in cells expressing wild-type mCherry-KCC2 and either mutant was reproducible and highly significant ($P < 0.01$).

Table 2. Predicted pathogenicity of the IGE *SLC12A5* (KCC2) variants. See also Supplementary Table S2.

Variant Name		Predicted Pathogenicity			
mRNA (NM_020708.4)	mRNA (NP_065759)	Mutation Taster		Panther	SIFT
c.2855 G>A	p.952 R>H	Disease causing*	*P* (probability): 0.7174	No prediction data	Not tolerated
c.3145 C>T	p.1049 R>C	Disease causing*	*P* (probability): 0.9999	$P_{deleterious}$ = 0.94634	Not tolerated

*Predicted specifically to disrupt the function of the last cytoplasmic domain.

We non-invasively corroborated these results by measuring KCC2-mediated Cl^- extrusion using Cl^--Sensor, a genetically encoded, ratiometric indicator of $[Cl^-]_i$ [25]. Cl^--Sensor was expressed in N2a cells with GlyR and WT or IGE variant mCherry-KCC2 (Fig 3A). Ratiometric recording of fluorescence was performed using excitation at 430 and 500 nm ($R_{430/500}$) [26]. Given the favorable weak endogenous Cl^--extruding mechanisms in N2a cells, once pre-loaded with Cl^- using a 3-minute co-application of KCl and glycine, N2a cells maintain a relatively elevated Cl^- level for more than 30 min [26] (Fig 3B). The mean ± s.e.m. half decay time of the fluorescence ratio was 26.7 ± 5.2 min, $n = 4$ (Fig 3D). In contrast to mock-transfected cells, cells expressing mCherry-KCC2 showed much faster ratiometric fluorescence recovery (see black trace in Fig 3B). The mean ± s.e.m. half decay time was 4.5 ± 0.4 min, ($n = 4$, $P < 0.01$, Fig 3D). Consistent with results obtained using gramicidin patch-clamp recording, mCherry-$KCC2_{R952H}$ or mCherry-$KCC2_{R1049C}$ resulted in a significantly slower recovery of the ratiometric fluorescence as compared to WT mCherry KCC2 (Fig 3B and D; Supplementary Table S4).

Measurements of the basal level of fluorescence ratio in cells expressing WT or IGE variant KCC2 constructs also supported our gramicidin-perforated patch results. Expression of mCherry-KCC2 produced a significant decrease in the basal level of $R_{430/500}$ from 1.16 ± 0.05 to 0.87 ± 0.01 arbitrary units (AU) (Fig 3B and C). Expression of mCherry-$KCC2_{R952H}$ or mCherry-$KCC2_{R1049C}$ produced intermediate values that were significantly lower than those measured with mCherry-KCC2 ($P < 0.05$ for both mutants) and did not differ from the control mock-transfected cells ($P > 0.05$; Fig 3C, Supplementary Table S5). Thus, both identified IGE KCC2 mutants extrude Cl^- with much lower efficacy relative to WT KCC2, resulting in cells with a higher basal level of intracellular Cl^-, and consequently, less hyperpolarized responses to glycine.

We modeled the effects of the two IGE KCC2 variants in conditions mimicking their heterozygous nature by performing gramicidin-perforated patch-clamp recordings in cells expressing equal proportions of WT eGFP-KCC2 and either of the IGE variant mCherry-KCC2 constructs (see Supplementary Methods for details) (Fig 2D). Recordings were performed exclusively from cells showing both a green and red fluorescence signal of equivalent intensity. Similar to experiments in cells expressing KCC2 R952H alone (see Fig 2C), cells co-expressing WT KCC2 and KCC2 R952H exhibited significantly less hyperpolarizing values of E_{Gly} relative to WT KCC2 (Fig 2D; Supplementary Table S3). Cells co-expressing WT KCC2 and KCC2 R1049C also showed a trend toward less hyperpolarized E_{Gly} values; however, this was not statistically different from WT KCC2, and the variability coefficient was much higher (Fig 2D; Supplementary Table S3).

We next studied whether the identified IGE KCC2 variants exhibit alterations in KCC2 surface expression by expressing WT or IGE variant KCC2 constructs harboring a pHluorine tag in the second putative transmembrane domain of KCC2 (KCC2-pH_{ext}; see Supplementary Methods for details) in cultured hippocampal neurons (Fig 4). WT KCC2-pH_{ext} exhibited the expected strong membrane-localized fluorescence (Fig 4B; Supplementary Table S6); in contrast, no signal was detected in neurons expressing a control KCC2 construct harboring an eGFP tag on the intracellular N-terminal domain (eGFP-KCC2). Neurons expressing KCC2-pH_{ext} R1049C showed transporter membrane localization similar to neurons expressing WT KCC2-pH_{ext} (Fig 4B and C; Supplementary Table S5). In contrast, neurons expressing KCC2-pH_{ext} R952H exhibited a consistent >twofold decrease in surface KCC2-pH_{ext} signal (Fig 4B and C; Supplementary Table S5).

The regulatory phosphorylation of KCC2 is altered in several neurological disease models, resulting in impaired KCC2 function [reviewed in 10, 11]. The stimulatory phosphorylation of KCC2 serine 940 (S940) promotes KCC2 activity via effects on both intrinsic transporter activity and trafficking to the plasma membrane, depending on the cellular context [27]. Using phospho-specific antibodies [21, 27] in Western blot assays with lysates derived from HEK293 cells expressing WT or IGE-mutant KCC2 constructs (see Supplementary Methods for details), we found that both KCC2 R952H and R1049C exhibited a reproducible and significant >50% decrease in S940 phosphorylation compared to WT KCC2, despite having unaltered levels of total protein expression (Fig 5A and B). These results suggest IGE KCC2 variants exhibit impaired function in part from a decrease in stimulatory S940 phosphorylation.

Discussion

The significant enrichment of KCC2 C-terminal NS genetic variants in IGE cases relative to controls (Table 1); the evolutionary conservation of the involved residues (Fig 1B and C); the predicted pathogenicity of their alteration in IGE (Table 2); and the impact of the detected IGE KCC2 variants on transporter function, trafficking, and/or S940 regulatory phosphorylation (Figs 2, 3, 4 and 5) suggest that genetically encoded impairment of KCC2 functional regulation might be a risk factor or contribute to the pathogenesis of human IGE. Notably, while our paper was in revision, Puskarjov et al [28] reported the KCC2-R952H variant co-segregating with febrile seizures in a single Australian family. In their study, KCC2-R952H was also shown to have reduced Cl^- extrusion capacity and decreased surface expression relative to WT KCC2. In addition, Puskarjov et al [28] showed KCC2-R952H has a compromised ability to induce dendritic spines. These data suggest that KCC2-R952H is also a susceptibility variant for febrile seizures in addition to IGE and further strengthen the genetic link between KCC2 and human epilepsy.

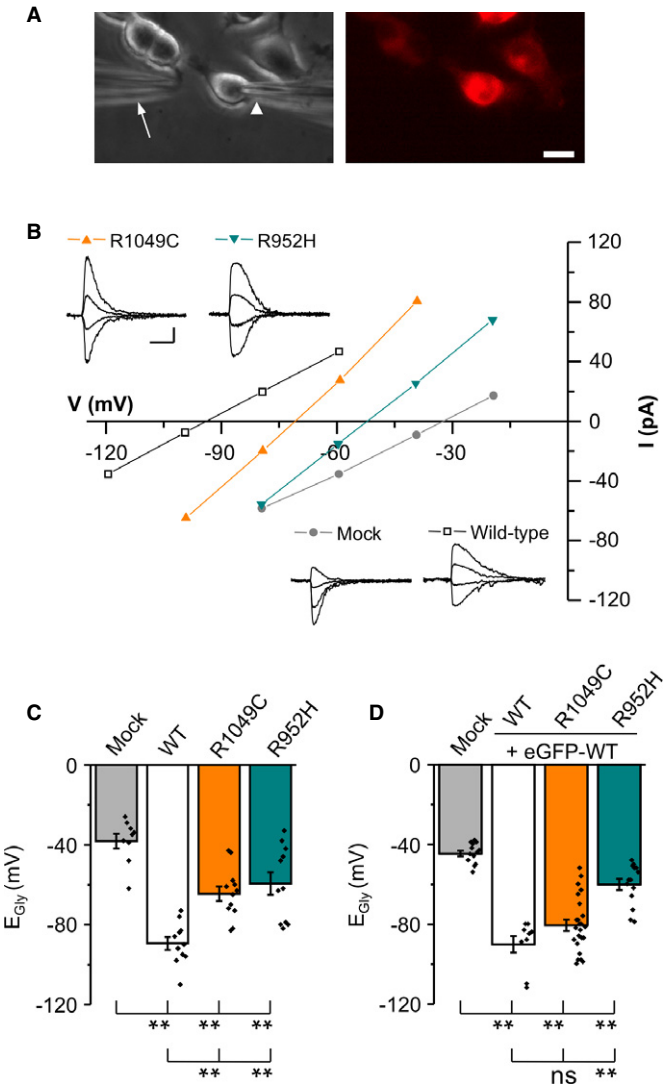

Figure 2. Effect of IGE variants on KCC2-dependent Cl^- reversal potential.

A Images of cells illustrating the position of the patch (arrowhead) and application pipette (arrow) used to deliver jet pulses of glycine (left). The mCherry-KCC2 positive cells were identified by their red fluorescence (right). Scale bar, 10 μm.

B Traces show examples of gramicidin patch-clamp recording obtained from N2a cells co-transfected with GlyR and an mCherry-KCC2 construct. Scale bars, 20 pA (vertical) and 500 ms (horizontal). Current amplitudes of GlyR currents (inset) were plotted against holding membrane potential. The current intercepts the voltage axis at E_{Gly}.

C Summary of all experiments similar to (B) (mean ± s.e.m., pooled data from 4 cultures, 2–3 cells per culture and condition). $^{**}P < 0.01$, one-way ANOVA test. Mock denotes cells transfected with mCherry and GlyR; see Supplementary Table S2 for detailed statistics.

D Summary of all experiments similar to B, but obtained from cells co-transfected with a 50:50 mixture of WT eGFP-KCC2 and one of the indicated mCherry-KCC2 IGE mutants (mean ± s.e.m., pooled data from 4 cultures, 5–8 cells per culture and condition). $^{**}P < 0.01$, one-way ANOVA test.

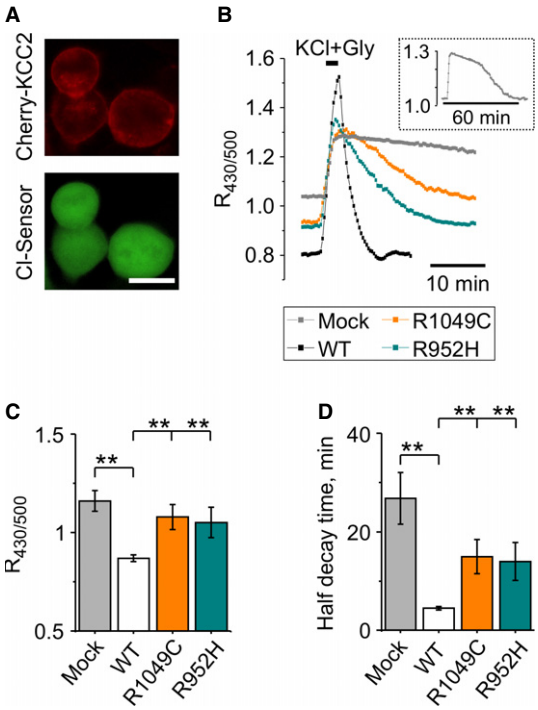

Figure 3. Effect of IGE variants on KCC2-mediated Cl^- extrusion capacity.

A Fluorescence signals recorded from N2a cells co-transfected with Cl-Sensor (green), GlyR (non-fluorescent), and mCherry-KCC2 (red, Obj 20×, NA 0.45, 500 nm excitation, scale bar = 20 μm).

B Representative traces of Cl-Sensor fluorescence ratio recording from N2a cells expressing different KCC2 constructs as indicated. Horizontal bar indicates the time of application of 100 mM KCl and 50 μM glycine. The ordinate axis indicates the ratio of Cl-Sensor fluorescence measured at 430 and 500 nm excitation wavelengths (R430/500). The inset illustrates the full record of R430/500 fluorescence from mock-transfected cells shown in the main plot.

C, D Columns show mean ± s.e.m. of the basal R430/500 level (C) and half decay time of Cl^- extrusion after glycine + KCl application (D). $n = 4 – 7$ experiments. $^{**}P < 0.01$, one-way ANOVA test (See Supplementary Tables S3 and S4 for details).

IGE is genetically heterogeneous, and the difficulty of identifying single variants as risk factors has been demonstrated by [9]. Heinzen *et al* did, however, report a list of variants that were found exclusively in IGE cases as potential risk factors (which did not include KCC2 variants), but suggested that the impact of an individual variant in IGE is small and that gene-based approaches might be more successful [9]. We have demonstrated that targeting a particular gene and taking a 'functional domain screening' approach, followed by detailed physiological validation, might be a complimentary approach in gaining insight into the genetic predisposition of IGE.

The empirical risk of IGE is compatible with an oligogenic cause of disease, suggesting that variants in multiple genes collectively contribute to the disorder [29–31]. Klassen et al [32] recently highlighted the complexity of IGE genetics. The authors noted that ion channel mutations are an important cause of disorders that affect the brain and other tissues so they decided to sequence 237 ion channel genes in 152 individuals with idiopathic epilepsy and 139 healthy controls. After developing variant profiles, three major conclusions were drawn: (i) complex combinations of common and rare ion channel variants are seen in epilepsy cases and controls;

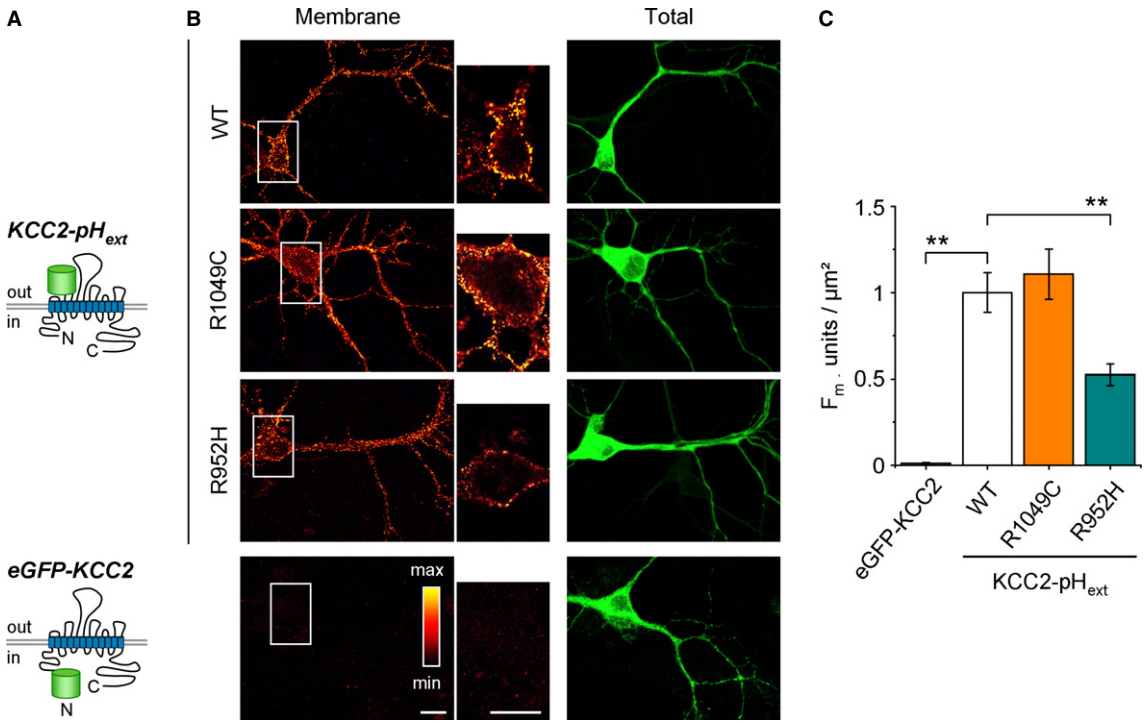

Figure 4. Effect of IGE KCC2 variants on KCC2 surface expression in rat primary hippocampal cultures.

A Schematic presentation of transfected constructs.

B Representative images illustrating surface labeling (left column) and total expression (right column) of WT KCC2-pH$_{ext}$ (top, raw image) and the R952H mutant of KCC2-pH$_{ext}$ (middle, raw image). As a control for the efficacy of surface labeling, we used a KCC2 construct with eGFP linked to the intracellular N-terminal domain (bottom, raw image). Scale bars, 20 µm.

C Normalized mean ± s.e.m. of the fluorescence intensity (Fm, left plot) of the surface-labeled KCC2-pH$_{ext}$ clusters (pooled data from 5 cultures, 5–8 cells per culture and condition). $^{**}P < 0.01$, one-way ANOVA test. (See Supplementary Table S5 for details).

(ii) healthy individuals carry variants in known epilepsy genes; and (iii) epilepsy individuals carry more than one variant in known epilepsy genes. Thus, the authors concluded that, in most cases, causality cannot be assigned to any one variant, but rather results from an individual's variant pattern, indicating an oligogenic mechanism [32]. They ultimately suggest that computational modeling of biologic networks is needed to improve risk predictions. Additionally, the authors state that these variant patterns can even explain the silencing of pathogenic alleles and why such variants (e.g., KCC2 R952H and R1049C) can be present in control individuals as well as inherited from unaffected parents [32]. Ultimately, population-based case/control studies are an approach that can implicate novel disease loci and provide a statistical measure of genetic risk. Studying a gene or gene region in this manner enables one to group variants together for statistical analysis, which minimizes multiple testing and makes it easier to reach levels of significance. Therefore, we conclude that NS variants in the C-terminus of KCC2 increases risk for IGE.

IGE KCC2 variants impair transporter Cl^- extrusion capacity and render E_{Gly} less hyperpolarized compared to WT KCC2 (Figs 2 and 3), consistent with *in silico* prediction models. Decreased KCC2-mediated Cl^- efflux in individuals carrying the IGE KCC2 variants would be anticipated to increase intracellular [Cl^-], raising the Cl^- reversal potential (E_{Cl}) to less hyperpolarized potentials and compromising $GABA_AR$- and/or GlyR-mediated hyperpolarizing inhibition. These effects of IGE KCC2 variants would be similar in nature, though much less potent in magnitude given their heterozygous state, to model organisms with complete knockout [2–5] or perhaps mild dysfunction (~30%) of KCC2 functional expression [33, 34], and humans with loss-of-function mutations in multiple $GABA_AR$ subunits in Mendelian IGE syndromes [35].

Our two IGE KCC2 mutants compromise KCC2 function likely by distinct mechanisms, including decreasing transporter plasmalemmal expression (R952H) or lowering the intrinsic activity of transporters at the cell surface (R1049C), consistent with the known trafficking-dependent and trafficking-independent mechanisms of KCC2 regulation encoded within the KCC2 C-terminus [10–12]. IGE KCC2 variants, by changing C-terminal protein structure, might alter the function of key regulatory domains (e.g., the so-called ISO domain, encoded in amino acids 1022-1037, which is required for isotonic KCC2-mediated hyperpolarizing GABAergic transmission [13]) by disrupting the binding of associated molecules. The significant inhibitory effect of R952H when co-expressed with WT KCC2 in a 1:1 ratio in neurons suggests a dominant-negative effect on transporter function, consistent with the known dimerization and oligomerization of KCC2 molecules [12,36]. Compared to R952H, a different mechanism is likely involved with R1049C, given results in 1:1 co-expression experiments.

Interestingly, both IGE mutants, despite having different effects on KCC2 trafficking, nonetheless exhibit decreased S940

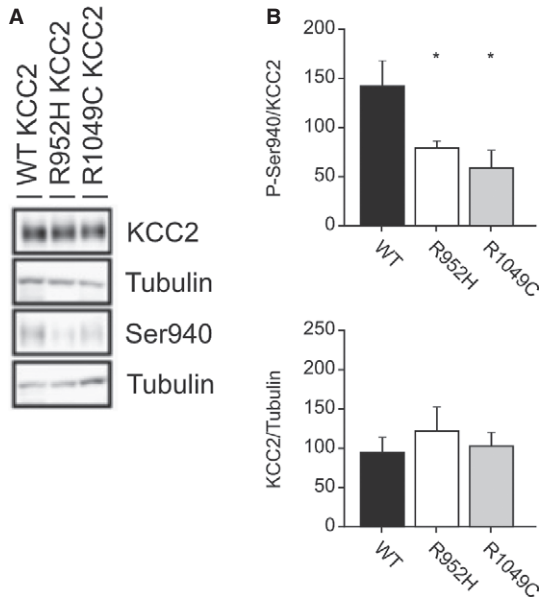

Figure 5. Effect of IGE KCC2 variants on serine 940 (S940) regulatory phosphorylation.

A HEK293 cells were nucleofected with the indicated WT, R952H, and R1049C KCC2 constructs. After 3 days, cells were lysed, and Western blotting was performed using anti-phospho-S940 KCC2 and total anti-KCC2 antibodies, as described in Materials and Methods. A representative Western blot is shown.

B Quantification of total phosphorylation of S940 relative to total KCC2 expression for each construct. 4 separate nucleofections were performed. $*P < 0.05$, one-way ANOVA test; All pairwise multiple comparison procedures (Tukey's test). Error bars represent the mean ± s.e.m.

phosphorylation. This result is interesting, suggesting specific relevance for residue S940 in IGE pathogenesis. In this regard, it is notable that brief exposure to glutamate, which is associated with seizure activity in humans [37], causes a rapid inhibition of KCC2 activity via S940 dephosphorylation that results in a prolonged loss of hyperpolarizing $GABA_A$-mediated currents in cultured hippocampal neurons [27,38]. Further investigation into these mechanisms of KCC2 functional regulation and phosphorylation will be important topics of future detailed biochemical study and may reveal novel insights not only into IGE pathogenesis, but also into potential ways to modulate KCC2 activity for therapeutic benefit in treatment-resistant seizures [39,40] and possibly other pathologies [7,11].

Materials and Methods

Recruitment and diagnosis of affected individuals

A total of 380 individuals with idiopathic generalized epilepsy (IGE) from the Quebec population of Canada were studied. Ethics approval for the recruitment and genetic analysis of these individuals were granted by the ethics committee at the CRCHUM (Centre de recherche du Centre hospitalier de l'Université de Montréal) and Montreal Neurological Institute. Upon recruitment, informed consent was obtained from all participants and a blood sample was collected for the genetic analysis. Recruitment was based on a referral from a neurologist or pediatrician in Quebec, Canada. All patients were from the greater Montreal and Quebec City regions. The diagnosis of IGE was based on a detailed clinical interview, full neurological examination, and an electroencephalography (EEG) recording. Patients were diagnosed according to International League Against Epilepsy (ILAE) criteria [41].

Population Controls

A total of 475 unrelated individuals who were recruited to the Rouleau laboratory as Quebec population controls were Sanger sequenced during Phase 1 of the project following the same protocol as IGE cases. In an effort to validate the association that was identified in Phase 1, an additional 516 population control samples from the Rouleau laboratory were Sanger sequenced. Furthermore, 223 unrelated individuals with French-Canadian ancestry who have never been diagnosed with a neurodevelopmental or neurodegenerative disorder and were previously exome sequenced were used as additional controls [96 of the exome-sequenced samples were provided by the CARTaGENE project [42]; an additional 74 and 53 exome-sequenced samples were provided by the laboratories of Dr. Majewski and Dr. Guy Rouleau, respectively].

Data within the chromosome 20 interval between 44,683,555 and 44,685,942 base pairs (hg19) that correspond to the nucleotides in exons 21 25 [NM_020708.4] and encode the C-terminus of KCC2 (SLC12A5) (encompassing amino acids 894 1086 [NP_065759]) were analyzed for variants. Samples were captured using either the Agilent capture kits v3 and v4 or the Illumina TruSeq Exome Enrichment and TruSeq DNA LT Sample Prep v2 kits. Sequencing was performed using the Illumina Highseq2000 sequencing platform at the Genome Quebec Innovation Center achieving a sequencing coverage averaging 70X. Exome read files were aligned to the human reference genome (hg19) using Burrow's Wheeler Aligner (BWA). PCR duplicates were removed, and only properly paired and uniquely mapped reads were kept. Realignments around indels and recalibration were performed with GATK tools. The variants were called using SAMtools/BCFtools and annotated using Annovar.

Please see Supplementary Methods for further materials and methods.

Supplementary information for this article is available online: http://embor.embopress.org

Acknowledgements

KK is supported by a Harvard-MIT Neuroscience grant and the Manton Center for Orphan Disease Research at Children's Hospital Boston. GR is supported by the Canadian Institutes of Health Research.

Author contributions

KTK, NDM, BL, PAD, PA, JM, TZD, SJM, IM, and GAR conceived and designed the experiments. PC provided samples. KTK, NDM, PF, LS, BL, YS, PLT, CB, AL, DS, ADL, AH, HN, and IM performed the experiments. KTK, NDM, PF, LS BL, AK, YS, PLT, BW, DS, ADL, AH, PA, HN, JM, TZD, SJM, IM, and GAR analyzed the data. KTK, NDM, AK, PAD, BW, TZD, SJM, IM, and GAR wrote the manuscript.

Conflict of interest

The authors declare that they have no conflict of interest.

References

1. Blaesse P, Airaksinen MS, Rivera C, Kaila K (2009) Cation-chloride cotransporters and neuronal function. *Neuron* 61: 820 – 838
2. Tanis JE, Bellemer A, Moresco JJ, Forbush B, Koelle MR (2009) The potassium chloride cotransporter KCC-2 coordinates development of inhibitory neurotransmission and synapse structure in *Caenorhabditis elegans*. *J Neurosci* 29: 9943 – 9954
3. Bellemer A, Hirata T, Romero MF, Koelle MR (2011) Two types of chloride transporters are required for GABA(A) receptor-mediated inhibition in *C. elegans*. *EMBO J* 30: 1852 – 1863
4. Hekmat-Scafe DS, Lundy MY, Ranga R, Tanouye MA (2006) Mutations in the K^+/Cl^- cotransporter gene kazachoc (kcc) increase seizure susceptibility in Drosophila. *J Neurosci* 26: 8943 – 8954
5. Hekmat-Scafe DS, Mercado A, Fajilan AA, Lee AW, Hsu R, Mount DB, Tanouye MA (2010) Seizure sensitivity is ameliorated by targeted expression of K^+-Cl^- cotransporter function in the mushroom body of the Drosophila brain. *Genetics* 184: 171 – 183
6. Hubner CA, Stein V, Hermans-Borgmeyer I, Meyer T, Ballanyi K, Jentsch TJ (2001) Disruption of KCC2 reveals an essential role of K-Cl cotransport already in early synaptic inhibition. *Neuron* 30: 515 – 524
7. Kahle KT, Staley KJ, Nahed BV, Gamba G, Hebert SC, Lifton RP, Mount DB (2008) Roles of the cation-chloride cotransporters in neurological disease. *Nat Clin Pract Neurol* 4: 490 – 503
8. Gardiner M (2005) Genetics of idiopathic generalized epilepsies. *Epilepsia* 46(Suppl 9): 15 – 20
9. Heinzen EL, Depondt C, Cavalleri GL, Ruzzo EK, Walley NM, Need AC, Ge D, He M, Cirulli ET, Zhao Q *et al* (2012) Exome sequencing followed by large-scale genotyping fails to identify single rare variants of large effect in idiopathic generalized epilepsy. *Am J Hum Genet* 91: 293 – 302
10. Chamma I, Chevy Q, Poncer JC, Levi S (2012) Role of the neuronal K-Cl co-transporter KCC2 in inhibitory and excitatory neurotransmission. *Front Cell Neurosci* 6: 5
11. Kahle KT, Deeb TZ, Puskarjov M, Silayeva L, Liang B, Kaila K, Moss SJ (2013) Modulation of neuronal activity by phosphorylation of the K-Cl cotransporter KCC2. *Trends Neurosci* 36: 726 – 737
12. Medina I, Friedel P, Rivera C, Kahle KT, Kourdougli N, Uvarov P, Pellegrino C (2014) Current view on the functional regulation of the neuronal K^+-Cl^- cotransporter KCC2. *Front Cell Neurosci* 8: 27
13. Acton BA, Mahadevan V, Mercado A, Uvarov P, Ding Y, Pressey J, Airaksinen MS, Mount DB, Woodin MA (2012) Hyperpolarizing GABAergic transmission requires the KCC2 C-terminal ISO domain. *J Neurosci* 32: 8746 – 8751
14. Darman RB, Forbush B (2002) A regulatory locus of phosphorylation in the N terminus of the Na-K-Cl cotransporter, NKCC1. *J Biol Chem* 277: 37542 – 37550
15. Gimenez I (2006) Molecular mechanisms and regulation of furosemide-sensitive Na-K-Cl cotransporters. *Curr Opin Nephrol Hypertens* 15: 517 – 523
16. Loscher W, Puskarjov M, Kaila K (2013) Cation-chloride cotransporters NKCC1 and KCC2 as potential targets for novel antiepileptic and antiepileptogenic treatments. *Neuropharmacology* 69: 62 – 74
17. Kahle KT, Staley KJ (2012) Neonatal seizures and neuronal transmembrane ion transport. In *Jasper's Basic Mechanisms of the Epilepsies* [Internet], Noebels JL, Avoli M, Rogawski MA, Olsen RW, Delgado-Escueta AV (eds), 4th edn, pp 1 – 12. Bethesda, MD: National Center for Biotechnology Information (US)
18. Gamba G (2005) Molecular physiology and pathophysiology of electroneutral cation-chloride cotransporters. *Physiol Rev* 85: 423 – 493
19. Howard HC, Mount DB, Rochefort D, Byun N, Dupre N, Lu J, Fan X, Song L, Riviere JB, Prevost C *et al* (2002) The K-Cl cotransporter KCC3 is mutant in a severe peripheral neuropathy associated with agenesis of the corpus callosum. *Nat Genet* 32: 384 – 392
20. Boettger T, Rust MB, Maier H, Seidenbecher T, Schweizer M, Keating DJ, Faulhaber J, Ehmke H, Pfeffer C, Scheel O *et al* (2003) Loss of K-Cl co-transporter KCC3 causes deafness, neurodegeneration and reduced seizure threshold. *EMBO J* 22: 5422 – 5434
21. de Los Heros P, Alessi DR, Gourlay R, Campbell DG, Deak M, Macartney TJ, Kahle KT, Zhang J (2014) The WNK-regulated SPAK/OSR1 kinases directly phosphorylate and inhibit the K^+-Cl^- co-transporters. *Biochem J* 458: 559 – 573
22. Kahle KT, Rinehart J, Lifton RP (2010) Phosphoregulation of the Na-K-2Cl and K-Cl cotransporters by the WNK kinases. *Biochim Biophys Acta* 1802: 1150 – 1158
23. Rinehart J, Maksimova YD, Tanis JE, Stone KL, Hodson CA, Zhang J, Risinger M, Pan W, Wu D, Colangelo CM *et al* (2009) Sites of regulated phosphorylation that control K-Cl cotransporter activity. *Cell* 138: 525 – 536
24. Pellegrino C, Gubkina O, Schaefer M, Becq H, Ludwig A, Mukhtarov M, Chudotvorova I, Corby S, Salyha Y, Salozhin S *et al* (2011) Knocking down of the KCC2 in rat hippocampal neurons increases intracellular chloride concentration and compromises neuronal survival. *J Physiol* 589: 2475 – 2496
25. Markova O, Mukhtarov M, Real E, Jacob Y, Bregestovski P (2008) Genetically encoded chloride indicator with improved sensitivity. *J Neurosci Methods* 170: 67 – 76
26. Friedel P, Bregestovski P, Medina I (2013) Improved method for efficient imaging of intracellular Cl(–) with Cl^- sensor using conventional fluorescence setup. *Front Mol Neurosci* 6: 7
27. Lee HH, Deeb TZ, Walker JA, Davies PA, Moss SJ (2011) NMDA receptor activity downregulates KCC2 resulting in depolarizing GABAA receptor-mediated currents. *Nat Neurosci* 14: 736 – 743
28. Puskarjov M, Seja P, Heron SE, Williams TC, Ahmad F, Iona X, Oliver KL, Grinton BE, Vutskits L, Scheffer IE *et al* (2014) A variant of KCC2 from patients with febrile seizures impairs neuronal Cl^- extrusion and dendritic spine formation. *EMBO Rep* 15: 723 – 729
29. Steinlein OK (2004) Genetic mechanisms that underlie epilepsy. *Nat Rev Neurosci* 5: 400 – 408
30. Lu Y, Wang X (2009) Genes associated with idiopathic epilepsies: a current overview. *Neurol Res* 31: 135 – 143
31. Saint-Martin C, Gauvain G, Teodorescu G, Gourfinkel-An I, Fedirko E, Weber YG, Maljevic S, Ernst JP, Garcia-Olivares J, Fahlke C *et al* (2009) Two novel CLCN2 mutations accelerating chloride channel deactivation are associated with idiopathic generalized epilepsy. *Hum Mutat* 30: 397 – 405
32. Klassen T, Davis C, Goldman A, Burgess D, Chen T, Wheeler D, McPherson J, Bourquin T, Lewis L, Villasana D *et al* (2011) Exome sequencing of ion channel genes reveals complex profiles confounding personal risk assessment in epilepsy. *Cell* 145: 1036 – 1048
33. Woo NS, Lu J, England R, McClellan R, Dufour S, Mount DB, Deutch AY, Lovinger DM, Delpire E (2002) Hyperexcitability and epilepsy associated with disruption of the mouse neuronal-specific K-Cl cotransporter gene. *Hippocampus* 12: 258 – 268
34. Zhu L, Polley N, Mathews GC, Delpire E (2008) NKCC1 and KCC2 prevent hyperexcitability in the mouse hippocampus. *Epilepsy Res* 79: 201 – 212
35. Maljevic S, Krampfl K, Cobilanschi J, Tilgen N, Beyer S, Weber YG, Schlesinger F, Ursu D, Melzer W, Cossette P *et al* (2006) A mutation in the

GABA(A) receptor alpha(1)-subunit is associated with absence epilepsy. *Ann Neurol* 59: 983 – 987

36. Uvarov P, Ludwig A, Markkanen M, Soni S, Hubner CA, Rivera C, Airaksinen MS (2009) Coexpression and heteromerization of two neuronal K-Cl cotransporter isoforms in neonatal brain. *J Biol Chem* 284: 13696 – 13704
37. During MJ, Spencer DD (1993) Extracellular hippocampal glutamate and spontaneous seizure in the conscious human brain. *Lancet* 341: 1607 – 1610
38. Lee HH, Walker JA, Williams JR, Goodier RJ, Payne JA, Moss SJ (2007) Direct protein kinase C-dependent phosphorylation regulates the cell surface stability and activity of the potassium chloride cotransporter KCC2. *J Biol Chem* 282: 29777 – 29784
39. Deeb TZ, Maguire J, Moss SJ (2012) Possible alterations in GABAA receptor signaling that underlie benzodiazepine-resistant seizures. *Epilepsia* 53: 79 – 88
40. Deeb TZ, Nakamura Y, Frost GD, Davies PA, Moss SJ (2013) Disrupted Cl^- homeostasis contributes to reductions in the inhibitory efficacy of diazepam during hyperexcited states. *Eur J Neurosci* 38: 2453 – 2467
41. Anon (1989) Proposal for revised classification of epilepsies and epileptic syndromes. Commission on Classification and Terminology of the International League Against Epilepsy. *Epilepsia* 30: 389 – 399
42. Hodgkinson A, Idaghdour Y, Gbeha E, Grenier JC, Hip-Ki E, Bruat V, Goulet JP, de Malliard T, Awadalla P (2014) High-resolution genomic analysis of human mitochondrial RNA sequence variation. *Science* 344: 413 – 415

TABLE S1. KCC2 (*SLC12A5*) variants detected in the IGE cohort, and corresponding Exome Variant Server data.

Non-synonymous variants detected in the "hotspot"		Detection of variants in IGE cohort			Control data - Exome Variant Server							
					European American data				All data			
mRNA (NM_020708.4)	Protein (NP_065759)	Number of probands	Number of alleles	Allele frequency (%)	Number of alleles	Allele frequency (%)	p-value	Odds ratio	Number of alleles	Allele frequency (%)	p-value	Odds ratio
c.2855 G>A	p.R952H	5/380	5/760	0.66	6/8600	0.07	$1.09X10^{-3}$	9.42 CI_{95}[2.3-37.1]	7/13006	0.05	$2.97X10^{-4}$	12.22 CI_{95}[3.1-44.8]
c.3145 C>T	p.R1049C	3/380	3/760	0.39	0/8600	0.00	$5.39X10^{-4}$	Inf CI_{95}[4.7-Inf]	0/13006	0.00	$1.70X10^{-4}$	Inf CI_{95}[7.1-Inf]
Total number of non-synonymous alleles detected		8/380	8/760	-	14/8600	-	$2.20X10^{-4}$	6.46 CI_{95}[2.3-16.6]	19/13006	-	$7.67X10^{-5}$	7.20 CI_{95}[2.7-17.3]

TABLE S2. Clinical features of patients with *SLC12A5* (KCC2) variants.

Variant	Patient	Sex	Ethnicity	Febrile seizures	Onset afebrile seizure	Seizure Types	EEG	Photosensitivity
p.952 R>H	1	M	Unknown	Unknown	Unknown	IGE	Unknown	Unknown
	2	M	FC	No	14	GTC, Myoclonus	GSW, bilateral spikes temporal/central	No
	3	F	FC	No	Unknown	Generalized	Unknown	Unknown
	4	F	FC	No	21	GTC, Absences	Abnormal, anterior theta	No
	5	M	FC	No	20	GTC	Normal	Unknown
p.1049 R>C	6	F	FC	No	8	GTC, Absences, Myoclonus	Abnormal, GSW	No
	7	M	FC	No	3	GTC, Absences, Myoclonus	Unknown	Unknown
	8	M	FC	No	14	GTC, Absences	Normal, diffuse theta	No

EEG = Electroencephalogram, F = Female, FC = French Canadian, GSW = Generalized Spike and Wave, GTC = Generalized Tonic-Clonic, IGE = Idiopathic Generalized Epilepsy, M = Male.

Table S3. Results of the statistical analysis of E_{Gly} in N2a cells expressing different mCherry-KCC2 mutants. The mean and SEM values are shown in Figure 2. SD = standard deviation, SEM = standard error of the mean, CV = coefficient of variation.

E_{Gly}

	Mean	SD	SEM	Median	CV	n
Mock	-38.1	11.0	3.7	-35	-0.29	9
Wild-Type	-89.4	10.5	3.2	-90	-0.12	11
R1049C	-64.5	12.7	3.7	-64	-0.20	12
R952H	-59.4	18.9	5.7	-62	-0.32	11

***p* (One-way ANOVA between pairs of conditions)**

	Mock		Wild-Type		R1049C	
	F	*p*	F	*p*	F	*p*
Wild-Type	112.9	<0.001				
R1049C	24.9	<0.001	25.9	<0.001		
R952H	8.9	0.008	21.3	<0.001	0.6	0.45

TABLE S4. Results of the statistical analysis of half decay time of Cl- Sensor ratiometric fluorescence in N2a cells expressing different mCherry-KCC2 mutants. The mean and SEM values are shown in Figure 3. SD = standard deviation, SEM = standard error of the mean, CV = coefficient of variation.

Half Decay Time

	Mean	SD	SEM	Median	CV	n
Mock	26.8	10.5	5.2	28.2	0.39	4
Wild-Type	4.5	0.94	0.35	4.3	0.21	7
R1049C	15.0	6.9	3.5	12.6	0.46	4
R952H	14.0	7.7	3.9	11.9	0.55	4

***p* (One-way ANOVA between pairs of conditions)**

	Mock		Wild-Type		R1049C	
	F	*p*	F	*p*	F	*p*
Wild-Type	34.1	<0.001				
R1049C	3.5	0.1	16.8	0.003		
R952H	3.9	0.09	11.2	0.009	0.03	0.86

TABLE S5. Results of the statistical analysis of basal R430/500 fluorescence ratio of Cl^- Sensor in N2a cells expressing different mCherry-KCC2 mutants. The mean and SEM values are shown in Figure 3. SD = standard deviation, SEM = standard error of the mean, CV = coefficient of variation.

R430/500

	Mean	SD	SEM	Median	CV	n
Mock	1.2	0.10	0.05	1.16	0.09	4
Wild-Type	0.9	0.04	0.02	0.87	0.05	7
R1049C	1.1	0.13	0.06	1.07	0.12	4
R952H	1.1	0.15	0.08	1.09	0.15	4

***p* (One-way ANOVA between pairs of conditions)**

	Mock		Wild-Type		R1049C	
	F	***p***	**F**	***p***	**F**	***p***
Wild-Type	43.5	<0.001				
R1049C	0.9	0.36	16.7	0.003		
R952H	1.4	0.28	9.1	0.014	0.08	0.79

TABLE S6. Results of the statistical analysis of surface staining (F_M, arbitrary units). The mean and SEM values are shown in Figure 4. SD = standard deviation, SEM = standard error of the mean, CV = coefficient of variation.

E_M

	Mean	SD	SEM	Median	CV	n
EGFP	0.84	1.57	0.28	0.30	1.9	31
Wild-Type	100	69.7	11.46	85.3	0.7	37
R1049C	110.5	88.8	14.6	80.2	0.8	37
R952H	52.4	35.5	6.17	48.9	0.7	33

***p* (One-way ANOVA between pairs of conditions)**

	Mock		Wild-Type		R1049C	
	F	*p*	F	*p*	F	*p*
Wild-Type	120.8	<0.001				
R1049C	28.6	<0.001	0.32	0.57		
R952H	39.2	<0.001	12.5	<0.001	12.4	<0.001

Supplementary Methods

Sanger Sequencing

Primers were designed using Primer3 (http://frodo.wi.mit.edu/) to amplify the genomic DNA that encodes the C-terminus of KCC2 (*SLC12A5*) (encompassing amino acids 894–1086 [NP_065759] encoded by the nucleotides in exons 21–25 [NM_020708.4]), along with the homologous region in KCC3 (*SLC12A6*) (amino acids 979–1570 [NP_598408] encoded by exons 22-24 [NM_133647.1]), and the N-terminal regulatory region of NKCC1 cotransporter (*SLC12A2*) (amino acids 150–252 [NP_001037] encoded by c.446–756, the end of exon 1 [NM_001046]). Primer sequences are available upon request. Polymerase chain reactions (PCRs) were performed using the AmpliTaq Gold DNA Polymerase (Applied Biosystems, Foster City, California, USA) as per the manufacturer's instruction. To visualize DNA fragments, 5 µL of the PCR product was loaded on a 1% agarose gel. Ethidium bromide was used for the staining. PCR products were sequenced at the Genome Quebec Innovation Centre (Montréal, Québec, Canada) using a 3730XL DNAnalyzer (Applied Biosystems, Foster City, California, USA), and analyzed using the SoftGenetics program, Mutation surveyor (v.3.10, SoftGenetics, State College, Pennsylvania, USA).

Protein Sequence Alignment and In Silico Prediction Programs

Conservation of the KCC2 protein across species was determined by aligning the following orthologues: *Homo sapiens* (NP_065759), *Macaca mulatta* (XM_001104494.2_prot), *Rattus norvegicus* (NP_599190), *Mus musculus* (NP_065066), *Takifugu rubripes* (ENSTRUT00000047011) and *Danio rerio* (ENSDART00000009569). The effects of amino acid substitutions on protein function were predicted using MutationTaster, Panther, and SIFT.

Statistical Analysis

All statistical analysis for genetics was carried out using the program R (version 2.15.1). Fisher's exact test was used to generate the p-values and odds ratios.

Gramicidin perforated patch clamp recording

Gramicidin perforated-patch clamp recording was performed from N2a cells transfected with a mixture of two mammalian expression constructs in a modified Clontech backbone vector harboring the human α_1 subunit of the glycine receptor (GlyR), and N-terminal mCherry-tagged WT or IGE mutant KCC2. For control experiments, mCherry-KCC2 was substituted with an mCherry pcDNA construct (mock transfected cells). The transfection was performed using Lipofectamine 2000 according to manufacturer's protocol (Life Technologies SAS). Recordings were performed 48 to 56 h after transfection.

Coverslips with transfected N2a cells were placed onto the inverted microscope and perfused with an external solution (in mM): 140 NaCl, 2.5 KCl, 20 HEPES, 20 D-glucose, 2.0 $CaCl_2$, 2.0 $MgCl_2$, pH 7.4. Recordings were performed as described in [2, 3]. Briefly, the recording micropipettes (5 MΩ) were filled with a solution containing (in mM): 150 KCl, 10 HEPES, 20 mg/ml gramicidin A , pH 7.2. The tip of the pipette was filled with the same solution, but

without gramicidin. Glycine (50 µM) was dissolved in external solution and focally applied to soma and proximal dendrites through a micropipette (same as for patch clamp) connected to a Picospritzer (General Valve Corporation, pressure 5 p.s.i.) (**Figure 2A**). Recordings employed an Axopatch-200A amplifier and pCLAMP acquisition software (Axon Instruments) in voltage-clamp mode. Data were low-pass filtered at 2 kHz and acquired at 10 kHz. Input resistance (R_{in}) and capacitance were routinely determined from the analysis of responses to hyperpolarizing/depolarizing steps of − 10/+10 mV applied from the holding potential (V_h) of −60 mV. Before measurement of *I–V* relationships, a single test pulses was applied at V_h=-60 mV to determine the direction of I_{Gly} current, adjust the position of the pipette, and time agonist application with the final aim being to obtain short (300-1000 ms) current responses of low amplitude (less than -/+ 100 pA). Depending on the direction of current recorded at -60 mV, four glycine responses were recorded at voltages -120, -100, -80, -60 mV (for outwardly directed [positive] glycine-induced currents at -60 mV) or -80, -60, -40 and -20 mV (for inwardly directed [negative] glycine-induced currents at -60 mV) as shown in **Figure 2B**.

To test the function of heterozygote-like expression of KCC2 mutants, we co-expressed constructs encoding GlyR, eGFP-KCC2 into the N2a cells [2] and mCherry KCC2 in the proportions 1.4:1.0:1.0. For recordings, cells were chosen that showed similar intensities of eGFP and mCherry fluorescence by CCD camera acquisition and Metamorph software. The ranges of the fluorescence were identically set for all mutants.

Assay of KCC2 surface expression

In order to directly visualize the insertion of KCC2 IGE variants into the membranes of single neurons, we created a novel construct encoding KCC2 with a fluorescent tag introduced into the second extracellular loop of the transporter (KCC2-pH_{ext}; details provided on request). KCC2-pH_{ext} was transfected using a magnetofection kit after 10 days of *in vitro* primary culture of hippocampal neurons prepared from E19 rat embryos as described previously (Buerli et al., 2007). 48 h after transfection, neurons were rinsed with external solution containing in mM: 140 NaCl, 2.5 KCl, 20 HEPES, 20 D-glucose, 2.0 $CaCl_2$, 2.0 $MgCl_2$, pH 7.4 and incubated for 40 min at 18°C with polyclonal anti-GFP antibody (1:1000, Molecular Probes) dissolved in the same solution. The coverslips were rinsed x3 and fixed with Antigenfix (Diapath, Martingo, Italy) for 20 min (at RT), permeabilized with 0.3% Triton X-100, blocked by 5% goat serum, and labeled for 1h (RT) with a secondary CY3-congugated antibody. The images were acquired with an Olympus Fluorview-500 confocal microscope (40×; 1.0 NA). Quantitative analysis of KCC2-pH_{ext} surface labeling was performed using Metamorph software (Roper Scientific).

Assay of KCC2 phosphorylation status at S940

Detection of the phosphorylation state of S940 in cellular lysates expressing WT and IGE mutant KCC2 was performed essentially as described in detail in [4]. Briefly, HEK293 cells were cultured in DMEM with 10% FBS and 5%

penicillin/streptomycin, and transfected using the Biorad nucleofection system in OPTIMEM media per the manufacturer's instructions. After 2 days to allow sufficient expression, cells were lysed in 1X RIPA lysis buffer supplemented with protease and phosphatase inhibitors and subjected to SDS-PAGE. Millipore α-KCC2 antibody was used to detect total KCC2, and a phospho-specific antibody directed against S940 [4] was utilized to detect the phosphorylation state at this residue, as previously described.

Ratiometric Cl-Sensor imaging

Ratiometric imaging of Cl-Sensor fluorescence was performed from N2a cells transfected with a mixture of three mammalian expression constructs in a modified Clontech backbone vector harboring Cl-Sensor, the human α_1 subunit of the glycine receptor (GlyR), and an N-terminal mCherry-tagged WT or IGE mutant KCC2. For control experiments, mCherry-KCC2 was substituted with empty vector pcDNA3.1 (mock-transfected cells). Excitation of transfected cells was performed every 20 s through 500 (20) nm and then 430 (24) nm narrow-band excitation filters (referred to as 500 nm and 430 nm filters). Detailed sequences of constructs are available upon request; experimental procedures are provided in [3].

Three-dimensional Structure Modeling

The three-dimensional structure of human KCC2 C-terminal domain (CTD) was modeled by the I-TASSER [5] server with input KCC2 amino acid sequences 648 to 1116. Crystal structure of the cytoplasmic domain of a prokaryotic cation chloride cotransporter (PDB accession code 3G40) and several other structures were used as templates for comparative modeling. The top template 3G40 shows 26.67% sequence identity with KCC2 CTD. Among the five models predicted from the server, the one forming organized structure with a high C-score was chosen. The C-score of the modeled KCC2 CTD is -0.54, indicating high reliability and quality of the overall structural model. PyMOL was used for molecular graphics displaying.

REFERENCES

1. Hodgkinson A, Idaghdour Y, Gbeha E, Grenier JC, Hip-Ki E, Bruat V, Goulet JP, de Malliard T, Awadalla P (2014) High-resolution genomic analysis of human mitochondrial RNA sequence variation. *Science* **344:** 413–415

2. Pellegrino C *et al* (2011) Knocking down of the KCC2 in rat hippocampal neurons increases intracellular chloride concentration and compromises neuronal survival. *The Journal of Physiology* **589:** 2475-2496

3. Friedel P, Bregestovski P, Medina I (2013) Improved method for efficient imaging of intracellular Cl(-) with Cl-Sensor using conventional fluorescence setup. *Front Mol Neurosci* **6:** 7

4. Lee HH, Walker JA, Williams JR, Goodier RJ, Payne JA, Moss SJ (2007) Direct protein kinase C-dependent phosphorylation regulates the cell surface stability and activity of the potassium chloride cotransporter KCC2. *J Biol Chem* **282:** 29777-29784
5. Roy A, Kucukural A, Zhang Y (2010) I-TASSER: a unified platform for automated protein structure and function prediction. *Nat Protoc* **5:** 725-738

EMBO reports

Manuscript EMBOR-2014-38840

Genetically encoded impairment of neuronal KCC2 cotransporter function in human idiopathic generalized epilepsy

Kristopher T. Kahle, Nancy D. Merner, Perrine Friedel, Liliya Silayeva, Bo Liang, Arjun Khanna, Yuze Shang, Pamela Lachance-Touchette, Cynthia Bourassa, Annie Levert, Patrick A. Dion, Brian Walcott, Dan Spiegelman, Alexandre Dionne-Laporte, Alan Hodgkinson, Philip Awadalla, Hamid Nikbakht, Jacek Majewski, Patrick Cossette, Tarek Z. Deeb, Stephen J. Moss, Igor Medina and Guy A. Rouleau

Corresponding author: Guy A. Rouleau, Montreal Neurological Hospital and Institute, McGill University

Review timeline:

Submission date:	27 March 2014
Editorial Decision:	14 April 2014
Revision received:	18 April 2014
Accepted:	23 April 2014

Transaction Report:

(Note: With the exception of the correction of typographical or spelling errors that could be a source of ambiguity, letters and reports are not edited. The original formatting of letters and referee reports may not be reflected in this compilation.)

Transfer Note:

This manuscript was transferred from another journal with anonymous referee reports. Given the reports and the related paper from Kaila's group that we have just published, we decided to contact a single referee only.

Editor: Esther Schnapp

1st Editorial Decision 14 April 2014

Thank you for the submission of your manuscript to EMBO reports. We have now received the comments from the referee who was asked to assess it, and I am happy to tell you that s/he supports publication of the study in EMBO reports.

Can you please address all the comments by this referee and send us a revised manuscript as soon as possible? Please also shorten the manuscript text, as the character count largely exceeds our limit. The revised manuscript may not exceed 30,000 characters (including spaces, references and figure legends) and 5 main plus 5 supplementary figures, which should directly relate to a corresponding main figure. The Results and Discussion sections can be combined, which may help to eliminate some redundancy that is inevitable when discussing the same experiments twice. Commonly used materials and methods can further be moved to the supplementary information, but please note that materials and methods essential for the understanding of the experiments described in the main text must remain in the main manuscript file.

Regarding data quantification, can you please specify the bars and error bars for figure 5B?

I look forward to receiving a revised version of your manuscript as soon as possible.

REFEREE REPORT:

Referee #1:

n this manuscript Kahle et al. provide evidence that KCC2 variants may contribute to idiopathic generalized epilepsy (IGE), while Pusjarkov et al. reported that R952H might be associated with febrile seizures. Kahle et al. reports on a second C-terminal variant (R1049C) in addition to R952H in patients with IGE. Only after increasing the number of controls, the association for one of the variants (R1049C) becomes significant ($p = 0.044$), while R952H comes close to significance ($p = 0.065$). Taken together the p value for C-terminal KCC2 variants (i.e. R952H and R1049C) becomes significant.

Although the authors have been partially scooped by Pusjarkov et al., the current manuscript strengthens the genetic link between epilepsy and KCC2.

Minor points:
Overall one can feel that the manuscript was written in a hurry!

Page 5 "Nevertheless, R952H is enriched in IGE cases when population stratification is addressed". What does this exactly mean?
Abstract: Is severe IGE correct? This is not reported in the description of the cohort in the "Materials and Methods" section.
Figure 2C,D: The labeling of significance levels is puzzling. What has been compared?
Figure 3: From the "Materials and Methods" section the description how surface expression and overall expression can be distinguished is difficult to follow for the uninformed reader.
Page 10: I would prefer to display the Western blots to demonstrate that total KCC2 expression is indeed similar to WT for both variants. For the analysis of the phosphorylation all individual blots which were used for the quantification should be displayed in the supplement.
References: Some of the references need to be edited!

1st Revision - authors' response 18 April 2014

Response to editor’s comment:

Can you please address all the comments by this referee and send us a revised manuscript as soon as possible? Please also shorten the manuscript text, as the character count largely exceeds our limit. The revised manuscript may not exceed 30,000 characters (including spaces, references and figure legends) and 5 main plus 5 supplementary figures, which should directly relate to a corresponding main figure. The Results and Discussion sections can be combined, which may help to eliminate some redundancy that is inevitable when discussing the same experiments twice. Commonly

used materials and methods can further be moved to the supplementary information, but please note that materials and methods essential for the understanding of the experiments described in the main text must remain in the main manuscript file.

We have drastically reduced the amount of text from > 49,000 to almost 30,000 characters (including spaces, references and figure legends). To do this, we have eliminated superfluous information, shortened the introduction and discussion, and moved a considerable amount of methods/materials (including standard techniques like gramicidin perforated patch experiments, Western blotting, etc.) to a Supplementary Methods and Materials section. The text and figure legends describe methods details in sufficiently for a good understanding of the paper, and the reader is directed to the Supplementary section when appropriate for further methodological detail.

Regarding data quantification, can you please specify the bars and error bars for figure 5B?

This has been clarified in Figure 5.

Response to referee

Referee #1:

In this manuscript Kahle et al. provide evidence that KCC2 variants may contribute to idiopathic generalized epilepsy (IGE), while Pusjarkov et al. reported that R952H might be associated with febrile seizures. Kahle et al. reports on a second C-terminal variant (R1049C) in addition to R952H in patients with IGE. Only after increasing the number of controls, the association for one of the variants (R1049C) becomes significant ($p = 0.044$), while R952H comes close to significance ($p = 0.065$). Taken together the p value for C-terminal KCC2 variants (i.e. R952H and R1049C) becomes significant.

Although the authors have been partially scooped by Pusjarkov et al., the current manuscript strengthens the genetic link between epilepsy and KCC2.

Minor points:
Overall one can feel that the manuscript was written in a hurry!

Page 5 "Nevertheless, R952H is enriched in IGE cases when population stratification is addressed". What does this exactly mean?

This sentence has been changed to "Nevertheless, R952H is enriched in these Quebec IGE cases compared to Quebec controls." We were trying to address the fact that despite R925H has a higher frequency in the Quebec population compared to other reported frequencies (in EVS) it is still enriched in the Quebec IGE cohort compared to the corresponding population controls.

Abstract: Is severe IGE correct? This is not reported in the description of the cohort in the "Materials and Methods" section.

"Severe" is not precise and has been removed; the definition of our IGE cases is provided in Supplementary Data

Figure 2C,D: The labeling of significance levels is puzzling. What has been compared?

The significance bar with 4 prongs compares WT, R1049C, and R952H relative to mock-transfected controls; the significance bar with 3 prongs compares R1049C and R952H to WT.

Figure 3: From the "Materials and Methods" section the description how surface

expression and overall expression can be distinguished is difficult to follow for the uninformed reader.

This has been clarified in the appropriate section that has also been moved to Supplementary Materials and Methods to meet the character limit of 30,000.

Page 10: I would prefer to display the Western blots to demonstrate that total KCC2 expression is indeed similar to WT for both variants. For the analysis of the phosphorylation all individual blots which were used for the quantification should be displayed in the supplement.

-See Figure 5A showing total KCC2 expression is the same for both KCC2 IGE variants.
-We feel the representative blots displayed in the figures, coupled with the bar graph summaries (e.g., 5a and 5b) is sufficient, the standard means of presentation, and how we have displayed this data in the past using the same antibody and techniques (Lee et al., 2007, JBC; Lee et al., 2011, Nat Neurosci).

References: Some of the references need to be edited!

Agreed. We have updated all references given the drastic cutting in words to meet the word limit (47,000 to 30,000 characters)

2nd Editorial Decision 23 April 2014

I am pleased to accept your manuscript for publication in the next available issue of EMBO reports.

Thank you for your contribution to EMBO reports and congratulations on a successful publication. Please consider us again in the future for your most exciting work.

